Available online at www.sciencedirect.com
SCIENCE DIRECT®
C. R. Mecanique 333 (2005) 622–627
COMPTES RENDUS MECANIQUE
http://france.elsevier.com/direct/CRAS2B/

Mixing and coherent vortices in turbulent coaxial jets

Guillaume Balarac *, Mohamed Si-Ameur

L.E.G.I., B.P. 53, 38041 Grenoble cedex 09, France

Received 24 June 2005; accepted 28 June 2005

Available online 11 August 2005

Presented by Marcel Lesieur

Abstract

Direct numerical simulations associated with mixing in constant-density round coaxial jets are performed. They are validated by comparison against laboratory experiments. The mixing process is studied by seeding a passive tracer first in the outer annular jet, then in the inner jet. We demonstrate the important role played by coherent vortices in the mixing mechanisms. The turbulent mixing exhibits an intermittent character as a consequence of fluid ejections caused by the counter-rotating streamwise vortices. We quantify also the domination of the outer jet and show that the fluid issuing from the central jet remains confined. ***To cite this article: G. Balarac, M. Si-Ameur, C. R. Mecanique 333 (2005).***

Résumé

Mélange et tourbillons cohérents dans des jets coaxiaux turbulents. Nous développons des simulations numériques directes associées au mélange dans des jets ronds coaxiaux de densité uniforme. Ces simulations sont validées par comparaison avec des expériences de laboratoire. Le processus de mélange est étudié en introduisant un traceur passif dans le jet annulaire puis dans le jet central. Nous montrons le rôle important joué par les tourbillons cohérents dans les mécanismes du mélange. Le mélange turbulent présente un caractère intermittent qui est la conséquence d'éjections de fluide causées par les tourbillons longitudinaux contrarotatifs. Nous quantifions également la domination du jet extérieur et montrons que le fluide issu du jet intérieur reste confiné. ***Pour citer cet article : G. Balarac, M. Si-Ameur, C. R. Mecanique 333 (2005).***

Keywords: Turbulence; Computational fluid mechanics

Mots-clés : Turbulence ; Mécanique des fluides numérique

* Corresponding author.
E-mail addresses: guillaume.balarac@hmg.inpg.fr (G. Balarac), mohamed.si-ameur@hmg.inpg.fr (M. Si-Ameur).

1631-0721/$ – see front matter
doi:10.1016/j.crme.2005.07.003

1. Introduction

The main objective of the present work is focused on the study and analysis of the effect of the turbulent structures upon the scalar mixing process in free coaxial jets, which form when the streams issuing from the central and co-annular pipes meet and mix in the open environment. The specific interest of mixing studies in such a flow configuration lies in a wide range of industrial applications such as chemical engineering systems or combustion devices (in particular flames linked to flow characteristics in power-producing gas turbines).

Few research works available in the literature have considered the important problem of mixing in coaxial jets [1], and the numerical works were limited to an axisymmetric approximation [2].

Mixing-processes diagnostic or prediction entails thorough informations on the spatio-temporal scalar-field evolution, which are difficult to acquire within the frame of laboratory experiments, and cannot be obtained with the aid of turbulence closure models. Experiments permit high Reynolds numbers and may involve numerous species, but flow and scalar seeding parameters cannot be easily modified, especially as far as chemistry is concerned. On the other hand, direct numerical simulations give an exact information on temporal and spatial flow evolutions, and are a very efficient tool in reproducing flow coherent vortices [3] (which play a major role in mixing). However, they can model only a simplistic chemistry.

In this context, the present work provides a numerical investigation of the scalar mixing by means of Direct Numerical Simulation (DNS) in three-dimensional coaxial round jets. Section 2 gives a brief description of the numerical method. Section 3 presents the results, with emphasis put on relations between flow topological aspects and mixing-fraction field statistics.

2. Inflow conditions and numerical methods

The inlet-velocity profile shape is constructed with two 'hyperbolic-tangent' profiles. This is a good approximation to the inlet mean velocity in coaxial jets, and it allows a rigorous definition of the global flow parameters [3,4]. The velocity ratio between the outer and the inner jets is $r_u = 5$. The domain size is of $10.8D_1 \times 10.65D_1 \times 10.65D_1$ (where D_1 is the inner-jet diameter), along the streamwise (x) and the two transverse directions (y, z), respectively. The mixing of fluids issued from the inner and outer jets is studied through the mixing fraction f considered as a passive scalar. The Reynolds and Schmidt numbers are $Re = U_2 D_1/\nu = 3000$ (U_2 is the velocity of the outer jet) and $Sc = \nu/\kappa = 1$, respectively.

We solve numerically the full incompressible Navier–Stokes equations written in Cartesian coordinates in the parallelepipedic computational domain consisting in $231 \times 384 \times 384$ points with a uniform mesh size in all three directions. The spatial discretization is performed thanks to a sixth-order compact finite difference scheme in the streamwise direction, together with pseudo-spectral method in transverse and spanwise directions. Pressure–velocity coupling is ensured by a fractional step method, with a Poisson equation resolution to guarantee incompressibility. The time stepping is carried out with the aid of a third-order Runge–Kutta scheme. The outlet boundary condition is of a non-reflective type (see [3] for numerical details). The evolution of f is given by a advection–diffusion equation solved by a second-order semi-discretized TVD Roe scheme [5] for the spatial discretization of the advection term.

3. Results and discussion

Fig. 1(a) shows an instantaneous view of three-dimensional positive Q isosurfaces, in order to illustrate the flow structures. We recall that Q is the second invariant of the velocity-gradient tensor, and it is well recognized as a being a good indicator of coherent vortices [6]. The main features of the flow can be seen. Two types of primary vortices appear in the early transition stage ($x/D_1 < 3$): the inner and outer primary vortices. These

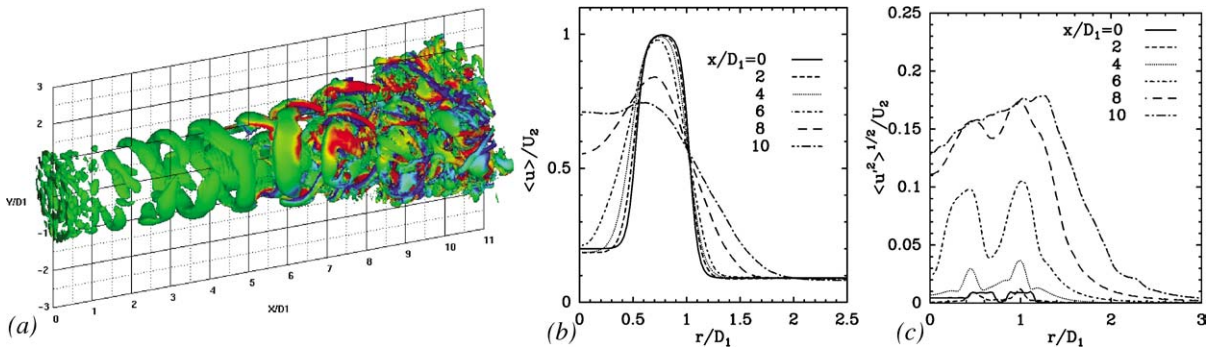

Fig. 1. (a) Isosurfaces of positive Q colored by the axial vorticity. (b) Mean axial velocity profiles at several downstream sections. (c) rms axial velocity profiles at several downstream sections.

Fig. 1. (a) Isosurfaces de Q positif colorées par la vorticité axiale. (b) Profils de vitesse axiale moyenne à plusieurs sections aval. (c) Profil de la fluctuation de la vitesse axiale à plusieurs sections aval.

vortices appear at each shear layer (between the inner and the outer jets and between the outer jet and the co-flow). They are a consequence of Kelvin–Helmholtz instabilities created by the inflexional shape of the upstream velocity profile. For coaxial jets with high velocity ratio ($r_u > 1$), they turn in opposite sense and a 'locking' phenomenon between the outer and the inner primary vortices implies that the inner and outer shear-layer shedding frequencies are equal [7]. Around $x/D_1 \approx 7$, pairs of alternate streamwise vortices appear between two consecutive outer and inner primary vortices, in agreement with the classical scenario of three-dimensionalization in free-shear layers. The streamwise vortices play a dominant role in the transition processes towards a fully-turbulent state, and their location is very dependent of the inlet conditions [4]. The apparition of streamwise vortices is finally followed by an abrupt increase in the level of small-scale turbulence. Then the flow quickly reaches a state of fully-developed turbulence. Indeed, the axial velocity component time-frequency spectrum computed at the downstream end of the computational domain has a $-5/3$ range over about one decade. Fig. 1(b) shows the mean axial velocity $\langle u \rangle$ profile at several downstream locations (brackets indicate a temporal averaging). At the beginning of transition, the jet keeps a profile similar to the inlet one. But downstream of $x/D_1 \approx 8$, the axial velocity profile loses its two-layer structure and the maximum velocity locates at the centerline. At the end of the computational domain, the most-intense turbulent activity is localized in the outer annular jet (Fig. 1(c)). Moreover, there is a 'pinching' of the central jet by the annular jet implying a shift of the outer potential core towards the jet center [4]. This phenomenon is due to a strong momentum transfer from the outer jet to the inner jet for a high velocity ratio. These last points reveal the outer-jet domination for high velocity-ratio coaxial jets.

In order to focus our analysis on scalar mixing, a 'numerical passive tracer' has been set up with two configurations. In the first case, we prescribe $f = 1$ in the outer stream and $f = 0$ elsewhere (inner stream and ambient fluid). The instantaneous planar flow along the central plane (Fig. 2(a)) gives a qualitative illustration of the mixing phenomena. The near-field region is quasi-linear until $x/D_1 = 4$. The consequence on the mean mixing fraction is that $\langle f \rangle$ remains equal to 0 and 1 in the inner and outer jet, respectively (Fig. 3(a)). Whereas the radial mixing fraction profiles indicate clearly a variation of $\langle f \rangle$ at the interfaces of the two fluids issued from the inner and outer jets (Fig. 3(b)). The mixing at this stage is mainly dominated by molecular diffusion, since a weak white-noise perturbation ($\approx 3\%$ of the fast outer stream) was introduced to let the instabilities develop naturally. Downstream of $x/D_1 = 4$, a turbulent mixing activity emerges as far as coherent structures become extensive. Fig. 2(b) shows the mixing-fraction isosurface $f = 0.5$. It is a good indicator of the mixing efficiency in the turbulent mixing conditions. Characterization of the multiscale geometry of the iso-species surfaces is a crucial step for understanding and modeling turbulent mixing linked to turbulent combustion processes. The isosurface $f = 0.5$ is highly convoluted after the instabilities amplification, with evidence of a large-scale structures. Thus, the turbulent mixing starts with an engulfment of the two jet fluids through the shear layers implied by the Kelvin–Helmholtz vortices.

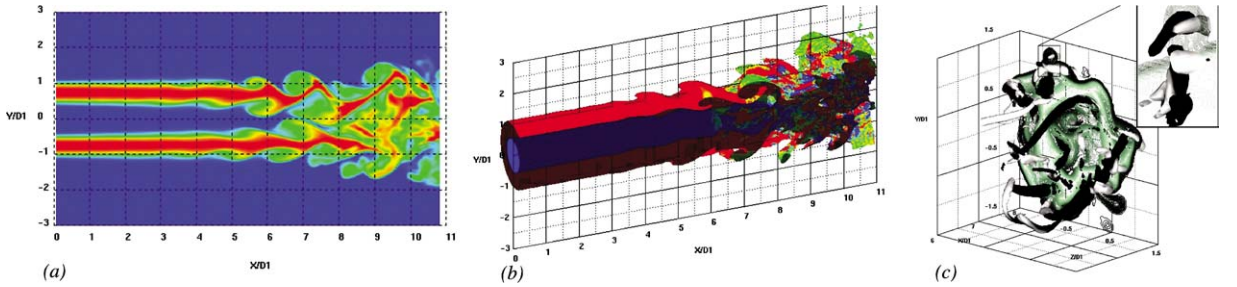

Fig. 2. (a) Instantaneous contours of mixing fraction in the central plane. (b) Cut view of mixing fraction isosurface ($f = 0.5$) coloured by the tangential vorticity. (c) Zoom of passive-scalar ejections by the counter-rotating longitudinal vortices (shown by an isovolume of $Q > 0$ coloured by the axial vorticity).

Fig. 2. (a) Contours instantanés de la fraction de mélange dans le plan central. (b) Vue coupée d'une isosurface de la fraction de mélange ($f = 0{,}5$) colorée par la vorticité tangentielle. (c) Illustration des éjections de scalaire passif par les tourbillons longitudinaux contrarotatifs (montrée par un isovolume de $Q > 0$ coloré par la vorticité axiale).

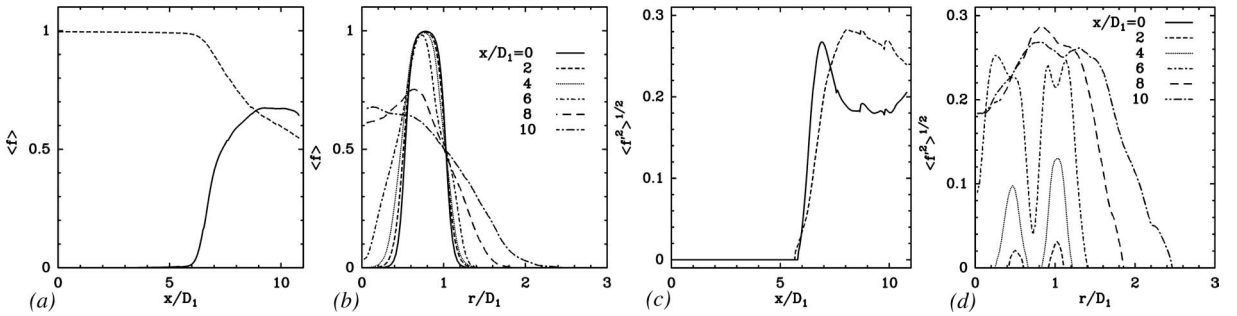

Fig. 3. Mean mixing fraction: (a) Downstream evolution in both central (continuous line) and annular jet (dashed line); (b) Radial evolution at several downstream locations. Mixing fraction rms: (c) Downstream evolution in both central (continuous line) and annular jet (dashed line); (d) Radial evolution at several downstream locations.

Fig. 3. Fraction de mélange moyenne : (a) Evolution longitudinale dans le jet central (ligne continue) et dans le jet annulaire (ligne pointillée) ; (b) Evolution radiale à différentes sections. Ecart-type de la fraction de mélange : (c) Evolution longitudinale dans le jet central (ligne continue) et dans le jet annulaire (ligne pointillée) ; (d) Evolution radiale à différentes sections.

It explains the two distinct peaks of the mixing-fraction rms $\langle f'^2\rangle^{1/2}$ (noted also f'), located in the inner and the outer shear layers, respectively (Fig. 3(d)). Notice that these peaks have been also detected in experiments [8] with same maximum values (around 0.25). Beyond $x/D_1 = 5$, the presence of coherent structures improves the mixing activity. This is shown by Fig. 3(a) and (b) indicating that the mean mixing fraction increases drastically inside the central jet to reach an asymptotic value around $f = 0.5$, as a consequence of the tracer invasion and diffusion within the inner jet. The two species are then approximately equipartitioned, and reasonably-uniformly distributed inside the shear layers. On Fig. 2(b), where the isosurface is colored by the tangential vorticity field, one can distinguish two noticeable features fulfilling $f = 0.5$. Before $x/D_1 \approx 7$, the two structures are wholly decorrelated, while for $x/D_1 > 7$ they are strongly distorted, allowing interpenetration of species issued from the jets and co-flow. This merging between the two mixing layers is caused by the streamwise counter-rotating vortices which bring three dimensionality to the jet. Indeed, these three-dimensional vortices eject the numerous space-coherent packets of tracer into the ambient fluid and the inner jet, leading to the mushroom-shaped tracer structures. Fig. 2(c) shows clearly this phenomenon. Thus turbulent mixing becomes predominant after this stage with an impressive growth of mixing fraction rms downstream of $x/D_1 \approx 6$ (Fig. 3(c)). Finally, for $x/D_1 > 8$, Fig. 3(b) shows that the mean mixing fraction is maximum in the jet center. Near the outflow, large amounts of tracer invade the central jet and the inner and outer mixing layers merge in order to create a single mixing zone similar to simple

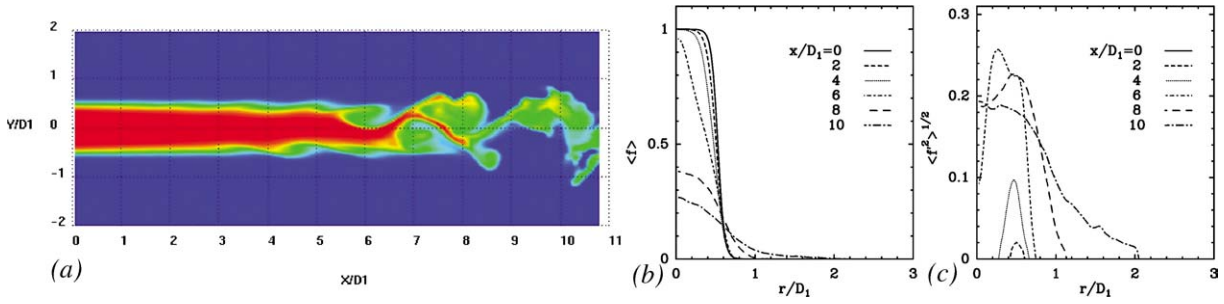

Fig. 4. (a) Instantaneous contours of mixing fraction in the central plane. (b) Radial evolution of the mean mixing fraction at several downstream locations. (c) Radial evolution of the mixing fraction rms at several downstream locations.

Fig. 4. (a) Contours instantanés de la fraction de mélange dans le plan central. (b) Evolution radiale de la fraction de mélange moyenne à différentes sections aval. (c) Evolution radiale de la fluctuation de la fraction de mélange à différentes sections aval.

jets. For the rms profiles of the mixing-fraction fluctuations (Fig. 3(d)), only the outer peak persists in this region. It is a consequence of the outer-jet dominance as far as mixing properties are concerned. Moreover, animations indicate that numerous spots of pure unmixed species are discernible at the end of the computational domain in the results corresponding to Fig. 2(a). They are the consequence of the mixing mechanism intermittent character. An appropriate time periodic forcing of three-dimensional longitudinal structures as well as vortical rings at the inlet boundary could decrease the amount of unmixed species and substantially increase the mixing.

In the last part of the study, we prescribe $f = 1$ in the inner jet and $f = 0$ elsewhere (annular jet and ambient fluid). In this second case, outer vortices do not contribute to the mixing because they do not transport tracer. The engulfment phenomenon is only in the inner shear layer. But the outer vortices hinder the radial development of the inner coherent vortices. Figs. 4(a) and 4(b) allow one to observe that the tracer remains confined between the edge and the centreline of the inner jet, with no more pure unmixed fluid from the inner jet beyond $x/D_1 = 5$. A large amount of fluid from the outer jet invades the inner jet generating mixing fraction values about 0.3–0.4, as a consequence of the domination implied by the outer jet. The peak of the mixing activity remains in the inner jet (Fig. 4(c)) with a weaker value (0.2 instead of 0.25 in the first case).

4. Conclusions

We have performed a study of mixing processes in round coaxial jets using direct numerical simulations. The mixing in flows consisting in an inner jet, annular jet and ambient fluid has been analysed with the aid of the spatio-temporal evolution of the mixing fraction (considered as a passive scalar) during the transition stages. We have shown the important role played by the coherent vortices in the turbulent mixing.

When the tracer is seeded in the annular jet, the turbulent-mixing process begins by an engulfment of species through both shear layers due to Kelvin–Helmholtz vortices. Further downstream, the turbulent mixing exhibits an intermittent character as a consequence of fluid ejections caused by the counter-rotating streamwise vortices. Moreover there is an important invasion of the fluid from the outer jet to the jet center due to the strong momentum transfer from the outer annular jet to the inner jet. Finally, spots of pure unmixed fluid persist in this configuration. This phenomenon represents a disadvantage for the mixing efficiency. This work suggests that an upstream control of the outer shear layer can decrease these amounts of unmixed fluid.

When the tracer is seeded in the inner jet, the mixing process is only due to the inner vortices. The tracer remains confined in the jet center because the outer vortices hinder the radial development of the inner streams. Finally, a large amount of fluid from the outer jet invades the inner jet. Thus, the mixing fraction value decreases strongly at the end of the transition in this mixing configuration.

Acknowledgements

Some of the computations were carried out at the IDRIS (Institut du Développement et des Ressources en Informatique Scientifique, Paris).

References

[1] E. Villermaux, H. Rehab, Mixing in coaxial jets, J. Fluid Mech. 425 (2000) 161–185.
[2] M.V. Salvetti, P. Orlandi, R. Verzicco, Effects of velocity ratio on vorticity dynamics and mixing in coaxial jet flow, in: 1st International Congress in Turbulent Shear Flows Phenomena, 2000.
[3] C.B. da Silva, G. Balarac, O. Métais, Transition in high velocity ratio coaxial jets analysed from direct numerical simulations, J. Turbulence 4 (2003) 24.
[4] G. Balarac, O. Métais, The near field of coaxial jets: a numerical study, Phys. Fluids, 17 (2005), in press.
[5] C. Hirsch, Numerical Computation of Internal and External Flows, vol. 2, John Wiley & Sons, 2002.
[6] Y. Dubief, F. Delcayre, On coherent vortex identification in turbulence, J. Turbulence 1 (2000) 11.
[7] G. Balarac, O. Métais, Coherent vortices in coaxial jets, in: CIMNE, Barcelona, 2004, pp. 149–152.
[8] B.D. Ritchie, D.R. Mujumdar, J.M. Seitzman, Mixing in coaxial jets using synthetic jet actuators, AIAA Paper, 2000-0404, 2000.